

NUCLEAR DATA AND MEASUREMENTS SERIES

ANL/NDM-39

**The Fission Cross Section of ^{239}Pu
Relative to ^{235}U from 0.1 to 10 MeV**

by

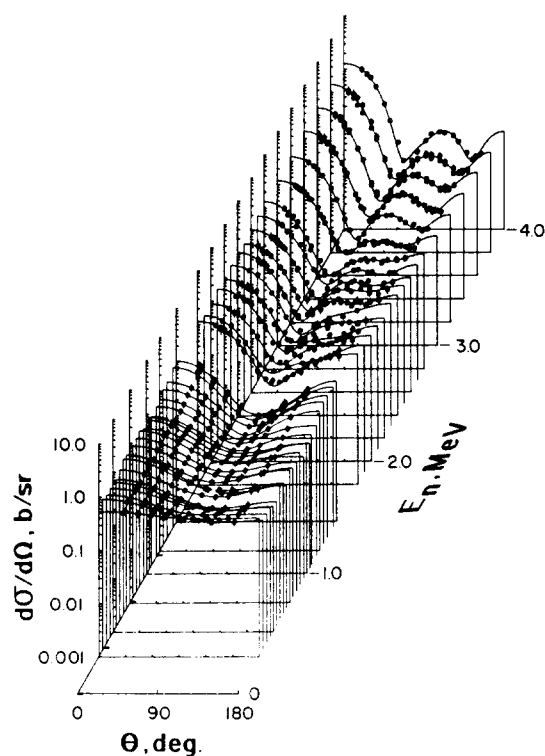
J.W. Meadows

March 1978

**ARGONNE NATIONAL LABORATORY,
ARGONNE, ILLINOIS 60439, U.S.A.**

NUCLEAR DATA AND MEASUREMENTS SERIES

ANL/NDM-39
THE FISSION CROSS SECTION OF ^{239}Pu RELATIVE TO
 ^{235}U FROM 0.1 TO 10 MEV
by
J. W. Meadows
Argonne National Laboratory
March 1978



ARGONNE NATIONAL LABORATORY,
ARGONNE, ILLINOIS 60439, U.S.A.

ANL/NDM-39
THE FISSION CROSS SECTION OF ^{239}Pu RELATIVE TO
 ^{235}U FROM 0.1 TO 10 MEV

by
J. W. Meadows
Argonne National Laboratory
March 1978

In October 1977, the U. S. Energy Research and Development Administration (ERDA) was incorporated into the U. S. Department of Energy. The research and development functions of the former U. S. Atomic Energy Commission had previously been incorporated into ERDA in January 1975.

Applied Physics Division
Argonne National Laboratory
9700 South Cass Avenue
Argonne, Illinois 60439
USA

NUCLEAR DATA AND MEASUREMENTS SERIES

The Nuclear Data and Measurements Series presents results of studies in the field of microscopic nuclear data. The primary objective is the dissemination of information in the comprehensive form required for nuclear technology applications. This Series is devoted to: a) measured microscopic nuclear parameters, b) experimental techniques and facilities employed in measurements, c) the analysis, correlation and interpretation of nuclear data, and d) the evaluation of nuclear data. Contributions to this Series are reviewed to assure technical competence and, unless otherwise stated, the contents can be formally referenced. This Series does not supplant formal journal publication but it does provide the more extensive information required for technological applications (e.g., tabulated numerical data) in a timely manner.

TABLE OF CONTENTS

	Page
ABSTRACT.	1
I. INTRODUCTION.	2
II. EXPERIMENTAL METHOD	2
III. THE ATOM RATIO.	2
IV. CORRECTIONS AND ERRORS.	4
V. DISCUSSION.	4
ACKNOWLEDGEMENTS.	5
APPENDIX.	6
REFERENCES.	9
TABLES.	10
FIGURES	14

THE FISSION CROSS SECTION OF ^{239}Pu RELATIVE TO
 ^{235}U FROM 0.1 TO 10 MEV*

by

J. W. Meadows
Argonne National Laboratory

ABSTRACT

The fission cross ratios of ^{239}Pu to ^{235}U were measured over the neutron energy range of 0.1 to 10 MeV. The atom ratios of the samples were based on their relative thermal fission rates and on their alpha activity.

*This work performed under the auspices of the U.S. Department of Energy.

I. INTRODUCTION

The fission cross sections of a number of uranium and plutonium isotopes are being measured relative to ^{235}U using the Argonne National Laboratory Fast Neutron Generator (FNG). The results for several uranium isotopes have been reported previously¹⁻⁴ as well as preliminary results for ^{239}Pu over a limited energy range.⁵ This report gives the final results for ^{239}Pu .

II. EXPERIMENTAL METHOD

Most of the aspects of the experimental system--basic method, apparatus, corrections, etc.--are described elsewhere¹⁻⁵ and are only summarized here.

The relative fission rates of samples of ^{239}Pu and ^{235}U which have well determined atom ratios are measured by placing them back-to-back in a double ionization chamber which is positioned perpendicular to the neutron beam axis. Neutrons with energies below 5 MeV are produced by the $^7\text{Li}(p,n)^7\text{Be}$ reaction. Higher energy neutrons are produced by the $\text{D}(d,n)^3\text{He}$ reaction using a gas target. A pulsed and bunched charged particle beam is used to obtain a pulsed neutron source and fast timing techniques select those fissions suitably correlated with the neutron burst.

Samples were prepared by electro-depositing thin layers of plutonium or uranium onto thin stainless steel plates. The ^{239}Pu deposit was of very high purity but the ^{235}U deposit contained enough ^{234}U to give a convenient alpha activity. The isotopic analyses are given in Table 1. Deposit diameters were 2.54 cm. The thickness of the plutonium deposit was $26 \mu\text{g Pu/cm}^2$. The uranium deposit was $162 \mu\text{g U/cm}^2$. Both deposits were converted to oxides.

III. THE ATOM RATIO

A critical quantity in this experiment was the measurement of the ratio of the number of atoms of fissionable material in the uranium sample to the

number of atoms in the plutonium sample. This was determined by two methods: (1) by the relative thermal fission rate and (2) by low geometry alpha counting.

The relative thermal fission rate was measured using the same detectors and electronics as was used for the measurements in the MeV range. Neutrons were thermalized in ~20 cm of paraffin wax surrounding the detectors. The primary neutron energy was 0.4-0.6 MeV. In order to remove the effect of the steep flux gradient in such an assembly several measurements were made with different detector orientations and these were averaged. The two assemblies used gave cadmium ratios for ^{235}U of 80 and 140. The atom ratio was calculated using the thermal fission cross sections listed in Table 2. Corrections were made for the non-Maxwellian spectral shape according to the method described by Westcott.⁶ An additional measurement was made in the thermal column of the Argonne Thermal Source Reactor (ATSR). This provided a well thermalized spectrum (the cadmium ratio for gold was 500) but the experimental arrangement, including the electronics, was entirely different. The results of the thermal fission measurements at the FNG and ATSR and the principal sources of error are listed in Table 3.

The alpha activities of the samples were measured in a low geometry alpha counter using a solid state detector with a resolution of 24 keV. Pulse-height spectra were taken for all counts and a window was set spanning the alpha peaks of the principal isotopes. The half-lives used to calculate the specific activities are given in Table 2. Several alpha counts were taken during the course of this measurement to check on possible loss of material from the samples. None was detected so all the counts were averaged and used to calculate the atom ratio given in Table 3.

IV. CORRECTIONS AND ERRORS

The principal corrections and errors are summarized in Table 4. The corrections for room and source background were measured for each point. Although the correction for a single detector could be large, it was similar for both detectors and the correction to the cross section ratio was usually small. The correction labeled *sample thickness* includes the sample thickness, fission fragment angular distribution and momentum transfer. These were considered in earlier measurements¹⁻⁵ but the correction has not been described in detail. This is done in Appendix A. The corrections for the neutron spectrum were quite small except near the high energy end of the range of each source reaction where neutrons from breakup reactions became significant. The neutron scattering correction considered only scattering from the detector and source structure. It was calculated using a procedure described in Ref. 11. The correction for the presence of other isotopes was small and the effect of any reasonable errors in the isotopic analysis was significant only in the measurement of the atom ratio. The combined identified systematic error ranges from 0.8 to 1.3%.

V. DISCUSSION

The results are listed in Table 5 and are compared to other measurements in Fig. 1. There have been a number of previous measurements of the $^{239}\text{Pu}:^{235}\text{U}$ fission cross section ratio. References 12-22 include only those measurements which have a major fraction of their data in the region between 0.1 and 10 MeV. Unnormalized shape measurements are also excluded. Only alternate points are plotted for Refs. 14, 17, 19, 20, and 22. However the total number of points to be plotted remains large so the comparison is made in three separate plots in order to keep them legible.

These results show few deviations from the general trend of the combined measurements. The agreement in the 1-4 MeV region appears good but below 1 MeV the present results are a little higher than most. The recent measurements of Carlson and Behrens²² cover the entire range of the experiment. In their normalization region (1.75-4.0 MeV) the average cross section differs from that of the present experiment by 0.7% while below 1 MeV there appears to be a systematic difference of about 1.3%. All this is well within the experimental errors. The only significant differences between the present work and that of Ref. 22 are in the 8-10 MeV region.

ACKNOWLEDGEMENTS

The author wishes to thank R. J. Armani for preparing the samples.

APPENDIX A

Corrections for Deposit Thickness, Momentum Transfer and Angular Distribution in Fission Detectors

It is assumed that (1) the detector contains a deposit of fissionable material of uniform thickness and radius which is oriented perpendicular to the direction of the incident particle, (2) all fragments emerging from the deposit are detected and (3) all fission fragments have the same range. At very low incident particle energies the fraction of undetected fissions is a function of the deposit thickness and the angular distribution. With increasing energy the angular distribution is given a forward bias which increases the loss in the backward direction and decreases the loss forward.

Consider the reaction



where M_1 is the incident particle, M_2 is the target nucleus and M_3 and M_4 are the fission fragments. The transformation of the angular distribution in the center-of-mass system, $\omega(\theta)$, to the laboratory system, $P(\theta_0)$, to the laboratory system, $P(\theta_0)$, is

$$P(\theta_0) = \frac{1 + \gamma^2 + 2\gamma \cos \theta}{|1 + \gamma \cos \theta|} \omega(\theta) \quad (2)$$

$$\tan \theta_0 = \frac{\sin \theta}{\gamma + \cos \theta} \quad (3)$$

$$\gamma = \left(\frac{M_1 M_3 E_{12}}{M_2 M_4 E_{34}} \right)^{1/2} \quad (4)$$

where θ_0 is the laboratory angle, θ is the center-of-mass angle, E_{12} is the energy due to the relative motion of M_1 and M_2 and E_{34} is the energy due to the relative motion of M_3 and M_4 . For neutron induced fission at energies of a few MeV, γ is quite small. At 30 MeV it is ~ 0.03 . As a result Eq. (3) reduces to

$$\tan \theta_0 \simeq \frac{\sin \theta}{\cos \theta},$$

θ may be replaced by θ_0 and the laboratory angular distribution can be approximated by

$$P(\theta_0) \simeq (1 + 2\gamma \cos \theta_0)\omega(\theta_0). \quad (5)$$

Fragments with a center-of-mass angle of $\pi/2$ will have a laboratory angle of

$$\theta_0 \simeq \pi/2 - \gamma \quad (6)$$

The fragment angular distribution is symmetric about $\pi/2$ in the center-of-mass system. In the laboratory system half the fragments will have angles between 0 and $(\pi/2 - \gamma)$ and half between $(\pi/2 - \gamma)$ and π . If the deposit faces the rear some fissions will not be observed because both fragments go forward. In the forward direction there is the possibility of detecting both fragments from some fissions. If the deposit is thin, i.e.

$$t < R \cos (\pi/2 - \gamma) \simeq R\gamma \quad (7)$$

where R is the fragment range, there will be no loss in the deposit.

The loss in the backward direction, L_B , may be expressed as 1 minus the fraction detected.

$$L_B = 1 - \frac{1}{t} \int_0^t dz \int_{-1}^{z/R} d \cos \theta_0 (1 + 2\gamma \cos \theta_0) \omega(\theta_0) \quad (8)$$

where z is the distance from the point of fission to the exit face of the deposit and t is the deposit thickness. There are two cases for L_F , the loss in the forward direction.

$$L_F = \frac{1}{t} \int_{R\gamma}^t dz \int_{\gamma}^{z/R} d \cos \theta_0 (1 + 2\gamma \cos \theta_0) \omega(\theta_0) \quad t > R\gamma \quad (9)$$

$$L_F = 0 \quad t < R\gamma \quad (10)$$

It is possible to express $\omega(\theta_0)$ as a series in $\cos^2\theta_0$. The first term is usually sufficient. The normalized angular distribution used in evaluating Eqs. (8) and (9) is

$$\omega(\theta_0) = (1 + b/3)^{-1} (1 + b \cos^2 \theta_0).$$

The integration of Eqs. (8) and (9) is straightforward but the result is lengthy. However, it has been assumed that $\gamma \ll 1$. If $t/R \ll 1$ then the higher order terms in these quantities may be dropped and the results reduce to

$$L_B \simeq (1 + b/3)^{-1} [t/2R + \gamma]$$

$$L_F \simeq (1 + b/3)^{-1} [t/2R + R\gamma^2/2t - \gamma] \quad t > R\gamma \quad (11)$$

$$L_F = 0 \quad t < R\gamma. \quad (12)$$

Another limiting case is the thick deposit where $t \geq R$. The effective value of t/R is 1. If γ is small

$$L_B \simeq (1 + b/3)^{-1} [1/2(1 + 2\gamma/3 + b/6 + \gamma b/5) + \gamma] \quad (13)$$

$$L_F \simeq (1 + b/3)^{-1} [1/2(1 + 2\gamma/3 + b/6 + \gamma b/5) - \gamma]. \quad (14)$$

REFERENCES

1. J. W. Meadows, Nucl. Sci. Eng. 49, 310 (1972).
2. J. W. Meadows, Nucl. Sci. Eng. 54, 312 (1974).
3. J. W. Meadows, Nucl. Sci. Eng. 58, 255 (1975).
4. J. W. Meadows, Nucl. Sci. Eng.
5. J. W. Meadows, Proceedings of the NEANDC/NEACRP Specialists Meeting on Fast Neutron Fission Cross Sections of U-233, U-235, U-238 and Pu-239, June 28-30, 1976, Argonne National Laboratory, ERDA-NDC-5/L.
6. C. N. Westcott, CRRP-787, Aug. 1958.
7. H. D. Lemmel, "The Third IAEA Evaluation of the 2200 m/sec and 20°C Maxwellian Neutron Data for U-233, U-235, Pu-239, and Pu-241," Conference on Neutrons Cross Sections and Technology, Washington, D. C., 1975, National Bureau of Standards Special Publication 425.
8. A. N. Jaffey, K. F. Flynn, L. E. Glendenin, W. C. Bentley and A. M. Essling, Phys. Rev. C4, 1889 (1971).
9. K. F. Flynn, A. H. Jaffey, W. C. Bentley, A. M. Essling, J. Inorg. Nucl. Chem. 34, 1121 (1972).
10. F. L. Oetting, Proc. Symp. Thermodynamics of Nuclear Materials with Emphasis on Solution Systems, Vienna, Austria (1967), IAEA, Vienna (1968).
11. D. L. Smith and J. W. Meadows, ANL/NDM-37, December 1977.
12. F. Netter, J. Julien, C. Corge and R. Ballini, J. de Physique 17, 556 (1956).
13. W. D. Allen and A. T. G. Ferguson, Proc. Phys. Soc. 70, 573 (1957).
14. G. N. Smirenkin, V. G. Nesterov and I. I. Bondarinko, Atomnaya Energiya 13, 366 (1962).
15. P. H. White and G. P. Warner, J. Nucl. Energy 21, 671 (1967).
16. V. G. Nesterov and G. N. Smirenkin, Atomnaya Energiya 24, 185 (1968); translation Soviet Atomic Energy 24, 224 (1968).
17. E. Pfletschinger and F. Kaeppler, Nucl. Sci. Eng. 40, 375 (1970).
18. W. P. Poenitz, Nucl. Sci. Eng. 40, 383 (1970).
19. M. Soleihac, J. Frehaut, J. Gauriau, and G. Mosinski, Second IAEA Conference on Nuclear Data for Reactors, Helsinki, 1970, IAEA, Vienna, 1970.
20. M. V. Savin, Yu. S. Zamyatnin, Yu. A. Khorhlov and I. N. Paramonov, "Fission Cross Section Ratios of ^{235}U , ^{239}Pu and ^{240}Pu for Fast Neutrons," INDC(CCP)-8U, p. 16, International Nuclear Data Committee (1970).
21. W. P. Poenitz, Nucl. Sci. Eng. 47, 228 (1972).
22. G. W. Carlson and J. W. Behrens, to be published in Nucl. Sci. Eng., May, 1978.

TABLE 1. Isotopic Analysis in Mole % of
the Samples Used in the Ratio
Measurements

Isotope	Sample	
	235-52	239-267
^{234}U	1.034	
^{235}U	98.409	
^{236}U	0.455	
^{238}U	0.102	
^{239}Pu		99.952
^{240}Pu		0.048

TABLE 2. The Alpha Half-lives and Thermal Fission Cross
Sections of the Uranium and Plutonium Isotopes

Isotope	$\sigma_{\text{th}}^{\text{a}}$ barns	$t_{1/2}$ years
^{234}U		$(2.447 \pm .002) \times 10^5{}^{\text{b}}$
^{235}U	$569.4 \pm 4.0{}^{\text{b}}$	$(7.038 \pm .005) \times 10^8{}^{\text{c}}$
^{236}U		$(2.341 \pm .002) \times 10^7{}^{\text{d}}$
^{238}U		$(4.468 \pm .003) \times 10^9{}^{\text{c}}$
^{239}Pu	$785.3 \pm 2.2{}^{\text{b}}$	$24290 \pm 70{}^{\text{b}}$
^{240}Pu		$6537 \pm 10{}^{\text{e}}$

^aCross sections averaged over a 20°C Maxwellian.

^bReference 37.

^cReference 8.

^dReference 9.

^eReference 10.

TABLE 3. Results of the Atom Ratio Measurements

	Thermal Ratio			Alpha Count
	FNG 1	ATSR	FNG 2	
Atom Ratio (U/Pu)	6.327	6.448	6.338	6.400
Average		6.321 \pm .060		6.400 \pm .053
Statistical Error	0.7	0.7	0.5	0.3
Thermal σ	0.48	0.48	0.48	
Sample Thickness	0.3	0.3	0.3	
Spectral Corr.	0.4	0.4	0.4	
Extrapolation	0.3	0.3	0.3	
Half-life				0.30
Mass Analyses	0.7	0.7	0.7	0.5
Counter Geometry				0.5
Grand Average		6.386 \pm .040		

TABLE 4. Summary of the Principal Corrections and Sources of Error

Correction/Error	Size of Correction (%)		Error in Ratio (%)
	Single Detector	Ratio	
Counting Statistics		0.5-5	
Room Background	~ 1	Negligible	0.5-5
Source Background	0-12	0-1	
Detector Efficiency			
Extrapolation	1-2	0.5	0.3
Sample Thickness	1.7-0.3	1.2-0.7	0.3
Neutron Spectrum		0-3	0-0.6
Neutron Scattering	4-8	0-0.5	0.1-0.2
Atom Ratio			0.65
Other Isotopes		~ 1	Negligible

TABLE 5. The $^{239}\text{Pu}:^{235}\text{U}$ Fission Cross Section Ratios

E_n (MeV)	ΔE_n (MeV) ^a	Ratio	Error in Ratio	
			Statistical	Total
.146	.016	.950		
.172	.012	1.068	.007	.011
.197	.014	1.074	.013	.015
.220	.012	1.100	.008	.012
.247	.013	1.136	.014	.016
			.008	.013
.268	.014	1.193		
.268	.037	1.169	.014	.017
.294	.014	1.243	.010	.014
.311	.016	1.237	.015	.018
.323	.031	1.241	.016	.019
			.010	.024
.336	.015	1.233		
.348	.015	1.284	.016	.019
.384	.029	1.263	.018	.021
.391	.029	1.315	.011	.015
.400	.018	1.302	.018	.021
			.065	.066
.452	.028	1.321		
.500	.027	1.347	.010	.015
.550	.024	1.367	.010	.015
.598	.032	1.402	.011	.016
.650	.030	1.392	.009	.014
			.013	.017
.687	.032	1.396		
.746	.030	1.453	.023	.026
.795	.032	1.518	.013	.018
.846	.030	1.484	.011	.017
.877	.039	1.472	.014	.019
			.012	.017
.943	.030	1.405		
.980	.038	1.406	.013	.017
.993	.026	1.445	.020	.023
1.045	.030	1.390	.012	.017
1.099	.023	1.417	.024	.027
			.011	.020
1.140	.046	1.453		
1.196	.022	1.440	.012	.017
1.234	.046	1.470	.011	.016
1.332	.044	1.531	.012	.017
1.429	.044	1.574	.012	.018
			.021	.025
1.526	.044	1.552		
1.622	.044	1.516	.020	.024
1.720	.044	1.476	.021	.024
1.818	.043	1.527	.020	.023
1.893	.072	1.522	.021	.024
			.016	.020

TABLE 5 (Contd.)

E_n (MeV)	ΔE_n (MeV) ^a	Ratio	Error in Ratio	
			Statistical	Total
1.924	.043	1.523	.021	.024
2.021	.043	1.580	.026	.029
2.232	.071	1.526	.010	.016
2.476	.070	1.490	.010	.016
2.729	.068	1.503	.011	.017
2.975	.068	1.515	.009	.016
3.226	.066	1.516	.011	.017
3.470	.066	1.551	.009	.016
3.719	.066	1.552	.008	.015
3.968	.066	1.540	.008	.015
4.221	.065	1.550	.014	.019
4.472	.065	1.545	.015	.020
4.702	.184	1.590	.011	.017
4.724	.064	1.578	.015	.021
4.972	.066	1.578	.018	.023
5.009	.167	1.596	.012	.018
5.300	.158	1.610	.012	.018
5.581	.152	1.632	.014	.019
5.852	.148	1.632	.013	.019
6.117	.147	1.580	.014	.019
6.414	.147	1.484	.013	.018
6.636	.146	1.404	.013	.017
6.895	.147	1.362	.013	.017
7.148	.148	1.347	.012	.016
7.402	.150	1.295	.011	.015
7.647	.149	1.289	.010	.015
7.870	.154	1.278	.011	.015
8.144	.156	1.338	.012	.016
8.390	.160	1.292	.011	.015
8.633	.162	1.291	.011	.015
8.876	.165	1.301	.012	.016
9.116	.168	1.283	.012	.016
9.360	.171	1.319	.011	.016
9.610	.175	1.293	.011	.017
9.840	.178	1.285	.011	.019

^a ΔE_n is one-half the full energy spread.

FIGURE CAPTION

Fig. 1a-1c. Measurements of the $^{239}\text{Pu}:^{235}\text{U}$ Fission Cross Section Ratio from 0.1-10 MeV.

